

Redox behavior of the molybdenum and tungsten metallafullerenes $M(\eta^2-C_{60})(CO)_2(phen)(dbm)$ ($phen = 1,10$ -phenanthroline; $dbm =$ dibutyl maleate): (spectro)electrochemistry and theoretical considerations

Piero Zanello,^{*,a} Franco Laschi,^a Marco Fontani,^a Carlo Mealli,^{*,b} Andrea Ienco,^b Kaluo Tang,^c Xianglin Jin ^{*,c} and Lei Li ^c

^a Dipartimento di Chimica dell'Università di Siena, Pian dei Mantellini, 44, 53100 Siena, Italy

^b ISSECC-CNR, Via Nardi 39, 50132 Firenze, Italy

^c Institute of Physical Chemistry, Peking University, Beijing 100871, P.R. China

Received 28th September 1998, Accepted 20th January 1999

Electrochemistry of $M(\eta^2-C_{60})(CO)_2(phen)(dbm)$ ($M = W$ **1**, Mo **2**; $phen = 1,10$ -phenanthroline; $dbm =$ dibutyl maleate) shows that the complexes undergo four sequential reduction processes. As with free C_{60} , the first three electrons add reversibly (even if the relevant potentials are shifted *ca.* 0.15 V toward negative values), whereas the fourth reduction features chemical irreversibility. Cyclic voltammetry gives evidence that, as a consequence of the latter process, the metal fragment decomplexes and $[C_{60}]^{3-}$ is released. In good agreement with this picture, a qualitative MO approach shows four close LUMOs for the ground state structure of the uncharged complexes. The first three levels are delocalized over C_{60} (somewhat extended to the dbm π system), while the fourth one is metal–fullerene antibonding (back donation $d_{\pi} \rightarrow \pi^* C_{60}$) and its occupation causes fulleride dissociation. The EPR spectra of the electrogenerated $[1]^-$ and $[2]^-$ monoanions are significantly different from that of $[C_{60}]^-$ and seem suggestive of metal character for these radical species. At present, this result is unexpected in that the unpaired electron in the anions $[1]^-$ and $[2]^-$ should be intuitively centered on the coordinated fullerene.

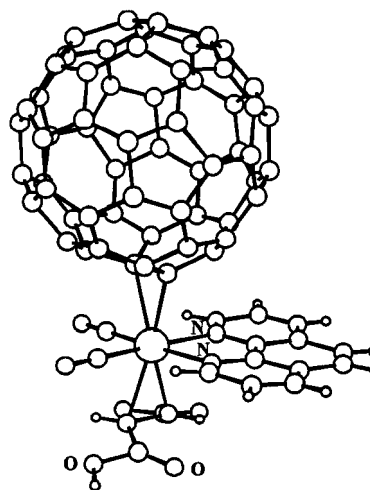
Introduction

The preparation and structural characterization of fullerene metal complexes, especially of C_{60} ¹ and C_{70} ,^{1,2} constitutes a growing field of research. From the electrochemical viewpoint, multiple electron transfer processes which have been shown to occur reversibly in free fullerenes³ have not equally encouraged exhaustive investigations on their transition metal adducts. In fact, the available data are still limited for C_{60} complexes,^{1,4} while, aside from a brief report,^{1f} there are no data for the C_{70} -analogs.

The effects of coordination on the electrochemical behavior of fullerenes may be summarized as follows. A metal is almost invariably dihapto linked to one [6:6] bond of C_{60} mainly owing to the significant back donation exerted by a filled d_{π} orbital into the olefin-type $C-C$ π^* moiety which is locally exhibited by both the t_{1u} and t_{1g} low lying LUMOs of fullerene.⁵ Even when the latter is uncoordinated, the high delocalization of the LUMOs induces any added electron density to spread over the carbon soccer ball so that multielectron reductions become progressively more difficult.⁴ In the presence of a metal fragment, one t_{1u} level is destabilized and, although the remaining levels are not directly involved in bonding interactions, an inductive effect reduces their capability to accept electrons with a concomitant shift of the redox potentials toward more negative values with respect to free fullerene. Conversely, the reductive process seems facilitated for the adduct between the bimetallic species $Fe_2S_2(CO)_6$ and C_{60} .^{1f} This case, which would require an *ad hoc* theoretical analysis, is intuitively different as the complexation at the [6:6] edge does not involve any metal atoms, rather the two sulfur bridges between them. Thus, the redox behavior of the coordinated fullerene requires a careful examination of the bonding capabilities of the metal fragment itself and the evaluation of the nature and energy of the frontier MOs.

We present here an electrochemical investigation performed

on two complexes of fullerene C_{60} with metals of Group VI, the structures of which have been recently characterized.^{1g} For illustrative purposes, a drawing of the species $M(\eta^2-C_{60})(CO)_2(phen)(dbm)$ ($M = W$ **1**, Mo **2**; $phen = 1,10$ -phenanthroline; $dbm =$ dibutyl maleate) is shown in Scheme 1.



Scheme 1

To the best of our knowledge, only a preliminary report on the electrochemical behavior of the $W(0)$ -fullerene complex $W(\eta^2-C_{60})(CO)_3(dppe)$ [$dppe = 1,2$ -bis(diphenylphosphino)ethane] has been reported.^{4c}

We judged it essential to present a qualitative description of the MO structure of the complexed fullerenes in order to derive a useful picture of the effects occurring when one or more electrons are added to these systems. At this time, the large nuclearity of the latter and the complicated magnetic properties

of the open shell anions essentially preclude sophisticated calculations. With the hope of elucidating the nature of the complex monoanions electrogenerated from **1** and **2**, their EPR spectra have been recorded and compared with the spectra of the free monofulleride ($[C_{60}]^-$). We find the interpretative arguments of the electrochemistry fairly reasonable, although the coupled EPR spectral data remain rather intriguing.

Experimental

General procedures

Anhydrous (99.9%), HPLC grade dichloromethane for electrochemical measurements was purchased from Aldrich. Electrochemical grade $[NBu_4][PF_6]$ from Fluka was used as the supporting electrolyte. Complexes **1** and **2** were prepared according to a recently reported procedure.^{1g} Complexes **3** and **4** were prepared as described below.

Cyclic voltammetry was performed in a three-electrode cell having a platinum disk working electrode (1.5 mm in diameter) surrounded by a platinum-spiral counter electrode and the aqueous saturated calomel reference electrode (SCE) mounted with a Luggin capillary. Low temperature measurements were performed under non-isothermic conditions.⁶ Either a BAS 100A electrochemical analyzer or a multipurpose Amel instrument (a Model 566 analog function generator and a Model 552 potentiostat) were used as polarizing units. Controlled potential coulometry was performed in an H-shaped cell with anodic and cathodic compartments separated by a sintered-glass disk. The working macroelectrode was a platinum gauze; a mercury pool was used as the counter electrode. The Amel potentiostat was connected to an Amel Model 558 integrator. Tests at low temperature were carried out by using an Ag/AgCl reference electrode. All the potential values are referred to the saturated calomel electrode (SCE). Under the present experimental conditions the one electron oxidation of ferrocene occurs at $E^\circ = +0.34$ V in the temperature range from -10 to $+10$ °C, and at $E^\circ = +0.35$ V at $+20$ °C. EPR measurements were performed on a BRUKER ER 200-SRDD spectrometer operating at X-band ($\nu = 9.78$ GHz). The operational microwave frequency (Bruker Microwave bridge ER 401 MR) was tested with an XL Microwave Frequency Counter 3120 and the external magnetic field H_0 was calibrated by using a dpph powder sample ($g_{dpph} = 2.0036$) (dpph = diphenylpicrylhydrazyl). The temperature was controlled with a Bruker ER 4111 VT device (accuracy of ± 1 °C). The samples were placed in a quartz tube positioned in the resonance cavity. Computer simulation of the EPR spectra was carried out by using the SIM14 A program.⁷

Syntheses

All the reactions were carried out under a dinitrogen atmosphere with the use of standard Schlenk techniques.

W(CO)₂(phen)(dbm)₂, 3. Dibutyl maleate (0.34 ml, 1.5 mmol) was added to a solution of $W(CO)_4(phen)^8$ (0.238 g, 0.5 mmol) in toluene (10 ml) and refluxed for 19 h. The solution was then concentrated and layered with light petroleum (bp 60–90 °C). After 7–10 days, the precipitated compound was filtered off, washed and dried *in vacuo* to give a yellow powder [0.320 g, 75% yield based on $W(CO)_4(phen)$]; mp 180.5–181.5 °C (Calc. for $C_{38}H_{48}O_{10}N_2W$: C, 52.06; H, 5.52; N, 3.20. Found: C, 52.19; H, 5.51; N, 3.13%). IR(KBr): ν_{max}/cm^{-1} 3429w, 3069w, 2958m, 2871m, 1964s, 1885s, 1726s, 1691s, 1602w, 1426m, 1259s, 1146s, 1022w, 849m, 738w, 558w, 458w, 390w.

Mo(CO)₂(phen)(dbm)₂, 4. Dibutyl maleate (0.5 ml, 2.2 mmol) was added to a solution of $Mo(CO)_4(phen)^8$ (0.260 g, 0.67 mmol) in toluene (12 ml) and refluxed for 17 h. The solution was then concentrated and layered with light petroleum (bp 60–90 °C). After 7–10 days, the precipitated compound was filtered

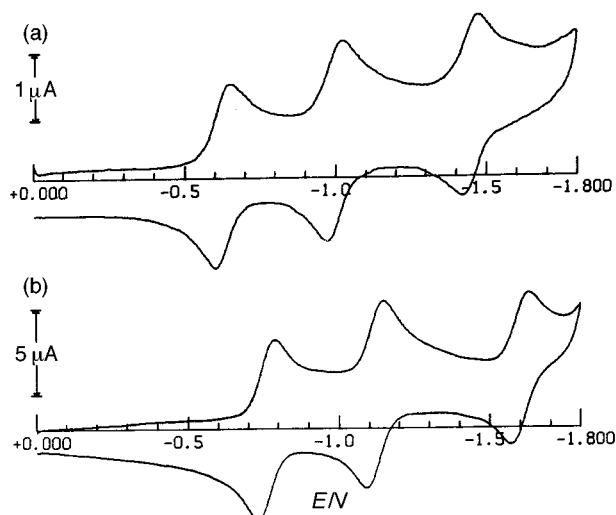


Fig. 1 Cyclic voltammetric responses at a platinum electrode recorded for CH_2Cl_2 solutions containing $[NBu_4][PF_6]$ (0.2 mol dm^{-3}) and: (a) C_{60} (saturated solution); (b) **1** ($6 \times 10^{-4} \text{ mol dm}^{-3}$). Scan rate 0.2 V s^{-1} , $T = -10$ °C.

off, washed and dried *in vacuo* to give a yellow powder [0.380 g, 72% yield based on $Mo(CO)_4(phen)$]; mp 127.6–128.4 °C (Calc. for $C_{38}H_{48}O_{10}N_2Mo$: C, 57.87; H, 6.13; N, 3.55. Found: C, 57.85; H, 6.16; N, 3.55%). IR(KBr): ν_{max}/cm^{-1} 3430w, 3070w, 2959m, 2872w, 1978s, 1914s, 1682s, 1455m, 1413m, 1287m, 1261m, 1155s, 1022w, 852w, 728w, 562w, 427w, 393w, 244w.

Computational details

In the MO calculations of the extended Hückel type⁹ a weighted-modified Wolfsberg-Helmholz formula¹⁰ was used. The literature STO parameters were used for Mo,¹¹ and the standard ones for the main group elements. The 3D drawings, correlation and interaction diagrams were performed with the program CACAO.¹²

Results and discussion

Electrochemistry

Fig. 1 shows a comparison of the cyclic voltammetric response of C_{60} and that of its adduct **1**, both recorded at -10 °C.

Paralleling previous electrochemical investigations on the related complex $W(\eta^2-C_{60})(CO)_3(dppe)$,^{4c} the metal fragment makes each reduction step shift towards more negative potential by *ca.* 0.15 V with respect to free C_{60} . The electrochemical reversibility of such reduction processes, as testified by their peak-to-peak separations, suggests that no significant structural reorganization accompanies the sequential addition of the three electrons with respect to that of the starting uncharged complexes.^{1g} Remarkably, even at the slow scan rate of 0.02 V s^{-1} ,¹³ the cyclic voltammogram of **1** does not suggest any evidence of the chemical complications observed for the reduction of $M(\eta^2-C_{60})(PR_3)_2$ ($M = Ni, Pd, Pt$),^{4a} thus indicating that in the present case the bonding of the metal fragment to the fullerene is much stronger. The same behavior is exhibited by complex **2**. The formal electrode potentials of the first three one-electron reductions of both complexes are compiled in Table 1, together with other results which will be discussed below.

Controlled potential coulometric tests ($E_w = -0.9$ V) confirm the one-electron nature of the first and subsequent reduction process of complexes **1** and **2**. In addition, cyclic voltammetry performed on the exhaustively one-electron reduced solutions affords voltammetric profiles complementary to the original ones, thus proving the chemical reversibility of the neutral/monoanion redox changes.

Table 1 Formal electrode potentials (V vs. SCE) and peak-to-peak separations (mV) for the redox changes exhibited by the metallafullerenes **1**, **2** and the related species **3**, **4**, in dichloromethane solution, at $-10\text{ }^{\circ}\text{C}^a$

Complex	$E^{\circ}(0/-)$	ΔE_p^b	$E^{\circ}(-/2-)$	ΔE_p^b	$E^{\circ}(2-/3-)$	ΔE_p^b	$E_p(3-/4-)^{a,c}$	$E_p(0/+)^{a,c}$
C_{60}	-0.63	59	-1.00	60	-1.45	64	-1.9 ^d	—
1	-0.76	62	-1.17	60	-1.60	62	-1.89	+0.98
2	-0.77	58	-1.13	58	-1.60	58	-1.89	+0.83
3	-1.60	90						+1.00
4	-1.67	88						+0.82 ^e

^a No significant differences have been obtained at $20\text{ }^{\circ}\text{C}$ (see text). ^b Measured at 0.2 V s^{-1} . ^c Peak potential value. ^d Difficult to be appreciated because of the partial overlapping with subsequent processes. ^e First of two almost overlapping irreversible oxidations.

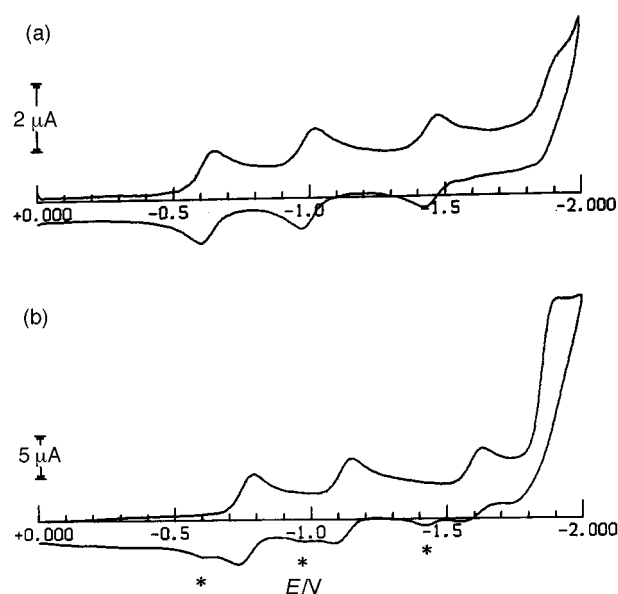


Fig. 2 Cyclic voltammetric responses recorded under the experimental conditions of Fig. 1, with scanings to values significantly more negative. (a) C_{60} ; (b) **1**.

Further elucidation of the redox propensity of the present complexes is provided by Fig. 2, which compares again the voltammetric profiles of free C_{60} and complex **1**, over a more extended cathodic window.

It shows that C_{60} undergoes a fourth one-electron reduction at about -1.9 V , which, because of the solvent discharge, features only partial chemical reversibility. Conversely at the same potential, complex **1** undergoes an irreversible reduction, likely involving a two-electron step. In this connection, it should be noted that the $\text{W}(0)$ precursor of complex **1**, i.e. complex **3**, undergoes a reduction process with features of chemical reversibility only at a very negative potential value ($E^{\circ} = -1.6\text{ V}$) and controlled potential coulometric tests investigating this cathodic process ($E_w = -1.8\text{ V}$) show the consumption of one-electron per molecule. Also in this case, the complete chemical reversibility of the process $[\mathbf{3}]^{0-}$ is confirmed in that, even at room temperature, the solution resulting from exhaustive reduction displays a cyclic voltammetric profile complementary to that of **3**.

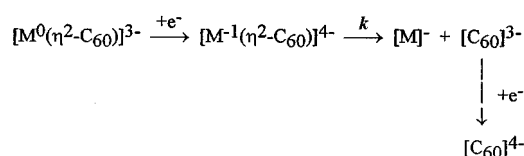
Complex **4** also undergoes, at room temperature, a one-electron reduction which is however complicated by slow degradation of the corresponding monoanion. By decreasing the temperature, the rate of the chemical degradation is slowed and, at $-20\text{ }^{\circ}\text{C}$, the i_{pa}/i_{pc} ratio attains unity already at 0.1 V s^{-1} .

Besides reduction, complexes **3** and **4** exhibit oxidation processes coupled to slow chemical complications.

Returning to complex **1**, the voltammogram of Fig. 2(b) not only indicates that the final reduction of complex **1** is irreversible, but also that decomplexation of C_{60} occurs and the reoxidation steps of free fullerene show up clearly in the backscan of Fig. 2(b) (starred peaks).

Thus, it is evident that in both **1** and **2**, the reduction of the

metal(0) fragment, although shifted by *ca.* $0.2\text{--}0.3\text{ V}$ with respect to the parent complexes **3**, **4** (Table 1), precedes the fourth one-electron reduction of the fullerene ligand (which should roughly manifest itself at about -2.05 V). Release of free $[\text{C}_{60}]^{3-}$ ensues which in turn undergoes the $3-/4-$ reduction. In summary, the most cathodic reduction should involve the chemical reaction given in Scheme 2 interposed between the two one-electron additions (ECE mechanism):



Scheme 2 $\text{M} = \text{W}/\text{Mo}(\text{CO})_2(\text{phen})(\text{dbm})$.

EPR spectroscopy

Before examining the EPR data obtained upon one-electron reduction of the fullerene complexes **1** and **2**, it should be taken into account that the low-temperature (263 K) electrogenerated monoanions $[\mathbf{3}]^-$ and $[\mathbf{4}]^-$ afford, at liquid-nitrogen temperature, EPR profiles, the resolved anisotropic features of which indicate axial symmetry with significant metal character ($g_{\parallel} > g_{\perp} \neq g_e = 2.0023$). There is no evidence of either hyperfine coupling of the unpaired electron with the magnetically active Mo or W nucleus [$I(^{95}\text{Mo}) = 5/2$; natural abundance = 15.7% ; $I(^{97}\text{Mo}) = 5/2$; natural abundance = 9.5% ; $I(^{183}\text{W}) = 1/2$; natural abundance = 14.4%], or superhyperfine coupling with the nitrogen nuclei of the *o*-phen ligand [$I(^{14}\text{N}) = 1$]. Upon raising the temperature, the intensity of the anisotropic signals progressively attenuate and disappear at the glassy-fluid transition. Upon refreezing, the axial signals are completely restored. The EPR parameters computed with best fit procedures are presented in Table 2.

Fig. 3 compares the liquid nitrogen ($T = 100\text{ K}$), first and second derivative, EPR spectra of the monoanion $[\text{C}_{60}]^-$ with that of its metallamonoanion $[\mathbf{1}]^-$, both electrogenerated in CH_2Cl_2 solution at 263 K .

In substantial agreement with previous findings on the electrogenerated $[\text{C}_{60}]^-$ in the same solvent,¹⁴ the spectra of $[\text{C}_{60}]^-$ [Fig. 3(a)] exhibit quasi-isotropic lineshapes with paramagnetic parameters which are consistent with the presence of a radical species displaying very minor orbital contribution: $g_{av} = 1.998(4)$; $\Delta H_{av} = 7.5 \pm 2\text{ G}$. As the temperature is increased beyond the glassy-fluid transition, the EPR signal further sharpens and, as a consequence of the effective averaging of the original anisotropic features in fast motion conditions, it becomes isotropic without appreciable *g* value changes in the whole range of fluid solution ($178\text{--}300\text{ K}$). This spectral behavior is reversible with temperature.

The liquid nitrogen spectra of $[\mathbf{1}]^-$ [Fig. 3(b)] exhibit a broad and axially resolved ($g_{\parallel} > g_{\perp} \neq g_e$) lineshape without hyperfine or superhyperfine resolution, which can be interpreted in terms of a $S = 1/2$ electron spin Hamiltonian. The result is most surprising as it seems to suggest that the unpaired electron has acquired a significant metallic character. In view of the

Table 2 Spectral EPR characteristics exhibited by the electrogenerated monoanions involved in the present study, at 100 K. $g_i = \pm 0.004$; $\Delta H_i = \pm 2$ G; $a_i = \pm 2$ G. ΔH_i and a_i in G

Anion	g_{\parallel}	g_{\perp}	$\langle g \rangle^a$	g_{av}	g_{iso}	ΔH_{\parallel}	ΔH_{\perp}	ΔH_{av}	ΔH_{iso}	a_{\parallel}	a_{\perp}
[3] [−]	2.050	2.007	2.021	—	—	15	20	—	—	≤15	≤20
[4] [−]	2.064	2.006	2.025	—	—	20	20	—	—	≤20	≤20
[C ₆₀] [−]	—	—	—	1.998	1.998 ^b	—	—	7.5	3.5 ^b	—	—
[1] [−]	2.095	2.007	2.036	—	—	22	20	—	—	≤22	≤20
[2] [−]	2.091	2.007	2.035	—	—	20	20	—	—	≤20	≤20

^a $\langle g \rangle = (g_{\parallel} + 2g_{\perp})/3$. ^b T = 200 K.



Fig. 3 X-Band EPR spectra recorded at 100 K on CH₂Cl₂ solutions of: (a) [C₆₀][−]; (b) [1][−]. Top: first derivative mode; bottom: second derivative mode.

composition of the LUMOs in **1** (overwhelmingly ligand-centered, *vide infra*), it is intriguing from the theoretical viewpoint to account for this. In addition, previous IR spectroscopic investigations on [Ir(η²-C₆₀)(CO)(η⁵-C₉H₇)][−] indicated no significant variation of the electronic structure of C₆₀, even if in that case the redox potential on complexation remained essentially unaltered (cathodically shifted by *ca.* 60 mV with respect to that of free fullerene).^{4b}

On the other hand, the fact that the spectrum is not an artifact seems to be supported by the fact that the typical isotropic EPR signal of [C₆₀][−] does not appear while recording the spectrum of the pure monoanion [1][−] at low temperature. Only upon holding the sample in the quartz tube under air and at room temperature does the anisotropic EPR signal disappear and the isotropic signal of [C₆₀][−] appear. A similar EPR behavior is exhibited by the electrogenerated monoanion [2][−]. All the relevant data are compiled in Table 2.

Qualitative MO considerations

The MO analysis follows the guidelines previously developed to evaluate the bonding capabilities of C₆₀ toward transition metal fragments.⁵

In general, a monometallic fragment with good d_π backbonding capabilities is able to coordinate a [6:6] edge of buckminsterfullerene in a dihapto fashion. The model is essentially that of a metal–olefin addition, *i.e.* donation of part of the C=C

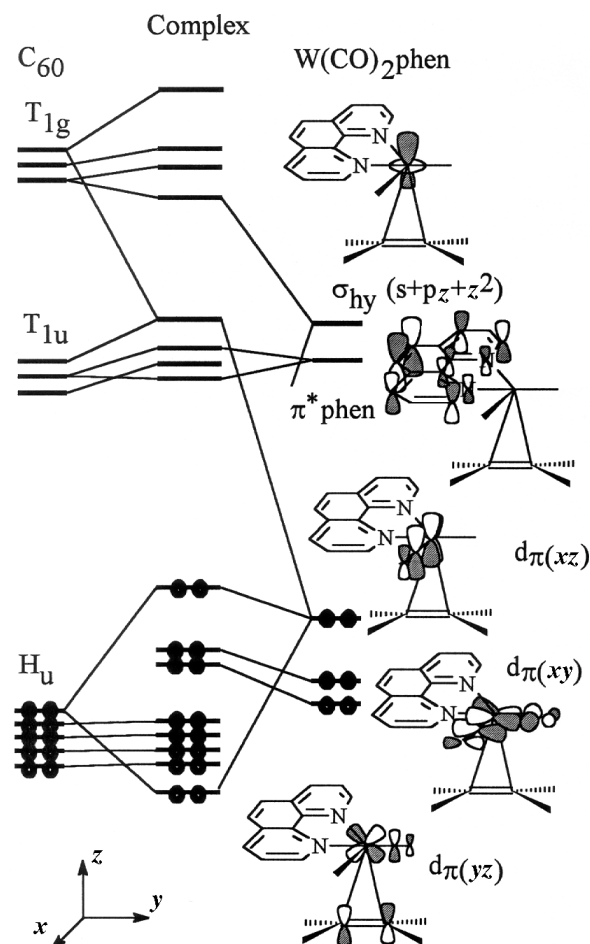


Fig. 4 Diagram showing the major orbital interactions between C₆₀ and the model fragment Mo(CO)₂(phen)(C₂H₄).

π bonding electron density into an empty σ hybrid of the metal and back donation from a filled d_π orbital into the C=C π* MO. The L₂M-d¹⁰ and L₅M-d⁶ metal fragments are known to be *isolobal*,¹⁵ a fact found in the few examples involved in C₆₀ coordination.^{1a} Accordingly, the basic MO picture of complexes **1** and **2** is not too different from that of the analogs containing the fragments (PR₃)₂M [M = Pd(0), Pt(0)].⁵ As a common structural feature, the coordinated [6:6] edge extends out of the quasi-spherical surface of the soccer ball. The diagram in Fig. 4 sketches the bonding interactions between C₆₀ and the square pyramidal model fragment Mo(CO)₂(phen)(C₂H₄).

On the left side, the two sets of triply degenerate LUMOs of the fullerene (T_{1u} and T_{1g}) are separated by <0.2 eV, while the HOMO–LUMO gap is estimated to be *ca.* 0.9 eV at our computational level. All of the higher MOs are at inaccessible energies.⁵ As is well known, the given triply degenerate pattern of the C₆₀ LUMOs is consistent with the easier addition of the first three electrons, although it has been shown that it is possible to add a second set of three electrons.³ Since the EHMO wave-

functions are monoelectronic, it is not surprising that the reduction potentials for each of the first three electrons are progressively more negative (see Table 1), in spite of their degeneracy. Any electron addition, after the first, is subject to correlations with those already present so that its addition costs more energy. The metal fragment, right side of Fig. 4, is square pyramidal although it has only approximate fourfold symmetry due to the different natures of the ligands. The metal carries six d electrons in the somewhat split 't_{2g}' orbitals. One of these, d_{yz}, is stabilized by the π^* level of the dbm olefinic moiety and by a π^* level of one CO ligand. The d_{xy} orbital lies at slightly higher energy and is stabilized by a pairwise combination of in-plane CO π^* orbitals, while d_{xz} is higher in energy interacting with only one CO ligand. For this reason, the latter is best suited for π -back donation into fullerene. It should be noted that each member of the C₆₀ LUMOs T_{1u} and T_{1g}, carries residual C–C π^* character at antipodal [6:6] edges, and hence is a potential π acceptor. Fig. 4 shows that two members from the T_{1u} and T_{1g} sets interact with d_{xz} and mix in the fourth LUMO L₄ where the π^* character of the coordinated C–C edge is partially cancelled out. This latter MO, which is depicted in the upper part of Fig. 5, is clearly metal–fullerene antibonding in character and, when populated, may induce separation between the metal fragment and the already reduced fullerene.

The MO treatment suggests why the three reversible reduction steps are comparable in number as well as essentially in potentials with those of the free fullerene while behavior begins to differ with the addition of the fourth electron. Upon complexation, of the T_{1u} members of C₆₀, one is unperturbed, one forms in-phase (L₁) and out-of-phase (L₃, in the lower part of Fig. 5) combinations with an accidentally degenerate π^* level of phenanthroline and only the third is destabilized by the metal d _{π} orbital (L₄). The L₁–L₃ energies compare with that of the original T_{1u} set and the fact that the electrons add to the system at potentials slightly more negative (*ca.* 0.15 V) may be related to the donor capabilities of the metal fragment itself. In fact, similar cathodic shifts were reported not only for the previously cited metallafullerenes,⁴ but also for the first and second reduction potentials of organofullerenes.¹⁶ It was found for the latter that the negative shifts are significantly reduced on passing from electron-donating to electron-withdrawing substituents. Accordingly, the cathodic shifts in the present case can be well justified on account of the significant metal back donation to C₆₀ upon coordination.

Fig. 4 shows that the HOMO of the complex is also significantly destabilized with respect to the other filled MOs, owing to a four-electron repulsion between one member of the H_u set (C₆₀ HOMO) and the d_{xz} orbital which is heavily involved in the major metal–C₆₀ back donation. This feature is typical for adducts of C₆₀ with L₂M–d¹⁰ fragments and is due to the residual π^* character at the coordinated [6:6] linkage exhibited by one member of H_u.⁵ It is indicated that, in order to mitigate the repulsion, the [6:6] linkage itself pulls out from the spherical surface of fullerene. The C–C π^* character at a given filled frontier MO is typically exhibited at the fusion edge between aromatic rings. The four-electron repulsion contrasts with the strength of the back donation itself. This effect has been judged particularly important for naphthalene which, contrary to C₆₀, is not known to coordinate a metal at its [6:6] fusion edge.¹⁷

Finally it is worth mentioning that the MO calculations for the species M(CO)₂(phen)(dbm)₂ (3 and 4) present, as the first LUMO, an uninvolved π^* level of the phenanthroline ligand (the same which in Figs. 4 and 5 is shown to mix with one C₆₀ LUMO). Almost degenerate with the latter, there are antibonding combinations between suitable metal d _{π} orbitals and the dbm π^* MOs. Since the character of the one-electron reduction varies from chemically reversible for 3 to partially chemically reversible for 4, it may be that the added electron ends up populating one of the latter metal–dbm antibonding MOs.

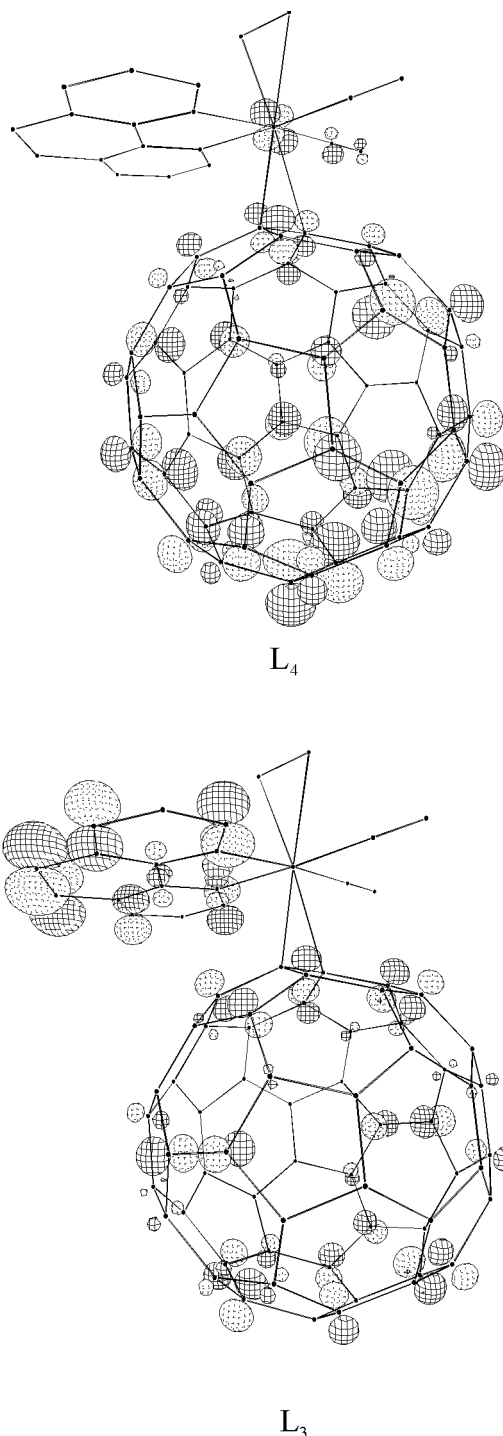


Fig. 5 CACAO drawings of the fourth and third LUMOs (L₄ and L₃) in the model complex Mo(η²-C₆₀)(CO)₂(phen)(C₂H₄). The upper picture shows the d _{π} [6:6] π^* of the level, while the lower one highlights the delocalization of the MO L₃ (of L₁ as well) over the C₆₀ and phen regions of the complex.

Consistent with EPR spectroscopy, a significant weakening of metal–olefin bonding could ensue with significant stabilization of a metal-centered orbital which hosts the unpaired electron. Finally, concerning the metal character of the unpaired electron in the monoanions [1][–], [2][–], differences with the spectra of [3][–], [4][–] are evident, hence it can be concluded that the same fragment [M(CO)₂(phen)(dbm)][–] might be generated upon reduction. Nevertheless, before assigning significant metal character to the paramagnetic anions [1][–] and [2][–], further evidence must be gained. We are planning to prepare multiple metalla-adducts of the type [M(CO)₂(phen)(dbm)]_n(η²-C₆₀) (*n* = 2, 3), the anions of which will likely enhance such metallic character.

Conclusions

The present investigation on the redox behavior of the fullerene complexes $M(\eta^2-C_{60})(CO)_2(phen)(dbm)$ ($M = W, Mo$) points out that, similarly to free C_{60} , up to three electrons can be added to the system with the features of chemical reversibility. The metal fragment, mainly bound through d_{π} back donation, pushes electron density into the fullerene so that its reduction processes $[C_{60}]^{0/-12/-13-}$ are shifted by about 0.15 V towards more negative potential values, without causing instability of the redox congeners. At variance with free fullerene, the addition of a fourth electron does not trigger further $[C_{60}]^{3-/4-}$ reduction, rather it produces a W/Mo monoanionic fragment which separates from the trianionic fulleride. In support of this, the MO analysis confirms that the fourth electron ends up populating the metal- C_{60} antibonding owing to the presence of an additional phenanthroline π^* level accidentally degenerate with the first set of C_{60} LUMOs.

The EPR spectra of the three electrochemically generated monoanion species, namely $[C_{60}]^-$, $[M(\eta^2-C_{60})(CO)_2(phen)(dbm)]^-$ and $[M(CO)_2(phen)(dbm)_2]^-$ appear substantially different from each other and their interpretation is not straightforward in all cases. The metallic character attributable to the unpaired electron in the monoanions $[3]^-$, $[4]^-$ is consistent with the reduction of the metal fragment itself given its reduced interaction with dbm ligands. As far as the anions $[1]^-$, $[2]^-$ are concerned, the electrochemical data indicate that the C_{60} remains strongly coordinated to the metal fragment, so that the unpaired electron is expected to delocalize over one MO of C_{60} , or, as suggested by the calculations, over a much larger region which extends also to the phenanthroline molecule. The present interpretation of the EPR data as due to some metal character of the unpaired electron is only provisional. Further investigations will be devoted in the near future to study in detail this apparently new aspect.

Acknowledgements

P. Zanello gratefully acknowledges the financial support by CNR of Italy and the technical assistance of Mrs G. Montomoli. K. Tang and co-workers acknowledge the financial support by National Natural Science Foundation of China (Project No. 29873001).

References

- (a) P. J. Fagan, J. C. Calabrese and B. Malone, *Acc. Chem. Res.*, 1992, **25**, 134; (b) J. M. Hawkins, *Acc. Chem. Res.*, 1992, **25**, 150; (c) R. Taylor and D. R. M. Walton, *Nature*, 1993, **363**, 685; (d) A. L. Balch, J. W. Lee, B. C. Noll and M. M. Olmstead, *Inorg. Chem.*, 1994, **33**, 5238 and references therein; (e) I. J. Mavunkal, Y. Chi, S.-M. Peng and G.-H. Lee, *Organometallics*, 1995, **14**, 4454 and references therein; (f) M. D. Westmeyer, T. B. Rauchfuss and A. K. Verna, *Inorg. Chem.*, 1996, **35**, 7140 and references therein; (g) K. Tang, S. Zheng, X. Jin, H. Zeng, Z. Gu, X. Zhou and Y. Tang, *J. Chem. Soc., Dalton Trans.*, 1997, 3585 and references therein; (h) K. Lee, H.-F. Hsu and J. R. Shapley, *Organometallics*, 1997, **16**, 3876 and references therein; (i) J. T. Park, H. Song, J.-J. Cho, M.-K. Chung, J.-H. Lee and I.-H. Suh, *Organometallics*, 1998, **17**, 227 and references therein; (j) H.-F. Hsu, Y. Du, T. E. Albrecht-Schmitt, S. R. Wilson and J. R. Shapley, *Organometallics*, 1998, **17**, 1756.
- A. L. Balch, D. A. Costa and M. M. Olmstead, *Chem. Commun.*, 1996, 2449 and references therein; H.-F. Hsu, S. R. Wilson and J. R. Shapley, *Chem. Commun.*, 1997, 1125.
- Q. Xie, E. Pérez-Cordero and L. Echegoyen, *J. Am. Chem. Soc.*, 1992, **114**, 3978; Y. Ohsawa and T. Saji, *J. Chem. Soc., Chem. Commun.*, 1992, 781; D. Dubois, G. Moninot, W. Kutner, M. T. Jones and K. M. Kadish, *J. Phys. Chem.*, 1992, **96**, 7137.
- (a) S. A. Lerke, B. A. Parkinson, D. H. Evans and P. J. Fagan, *J. Am. Chem. Soc.*, 1992, **114**, 7807; (b) R. S. Koefod, C. Xu, W. Lu, J. R. Shapley, M. G. Hill and K. R. Mann, *J. Phys. Chem.*, 1992, **96**, 2928; (c) J. R. Shapley, Y. Du, H.-F. Hsu and J. J. Way, *Recent Advances in the Chemistry and Physics of Fullerenes and Related Materials*, eds. K. M. Kadish and R. S. Ruoff, The Electrochemical Society, Pennington, NJ, 1994, vol. 24, p. 1255; (d) M. Iyoda, F. Sultana, S. Sasaki and H. Butenschön, *Tetrahedron Lett.*, 1995, **36**, 579; (e) J. T. Park, J.-J. Cho, H. Song, C.-S. Jun, Y. Son and J. Kwak, *Inorg. Chem.*, 1997, **36**, 2698; (f) A. N. Chernega, M. L. H. Green, J. Haggitt and A. H. H. Stephens, *J. Chem. Soc., Dalton Trans.*, 1998, 755.
- J. A. Lopez and C. Mealli, *J. Organomet. Chem.*, 1994, **478**, 161; N. Koga and N. Morokuma, *Chem. Phys. Lett.*, 1993, **202**, 230; H. Fujimoto, Y. Nakao and K. Fukui, *Inorg. Chem.*, 1980, **19**, 3068.
- M. P. Youngblood and D. W. Margerum, *Inorg. Chem.*, 1980, **19**, 3068.
- G. P. Lozos, B. M. Hoffman and C. G. Franz, *QCPE*, 1991, **23**, 20.
- M. H. B. Stiddard, *J. Chem. Soc.*, 1962, 4712.
- R. Hoffmann, *J. Chem. Phys.*, 1963, **39**, 1397; R. Hoffmann and W. N. Lipscomb, *J. Chem. Phys.*, 1962, **36**, 2179; R. Hoffmann and W. N. Lipscomb, *J. Chem. Phys.*, 1962, **37**, 3489.
- J. H. Ammeter, H.-B. Bürgi, J. C. Thibeault and R. Hoffmann, *J. Am. Chem. Soc.*, 1978, **100**, 3686.
- R. H. Summerville and R. Hoffmann, *J. Am. Chem. Soc.*, 1976, **98**, 7240.
- C. Mealli and D. M. Proserpio, *J. Chem. Educ.*, 1990, **67**, 399.
- E. R. Brown and J. R. Sandifer, *Physical Methods of Chemistry. Electrochemical Methods*, eds. B. W. Rossiter and J. F. Hamilton, Wiley, New York, 1986, vol. 2, ch. 4.
- T. Kato, T. Kodama, M. Oyama, S. Okazaki, T. Shida, T. Nakagawa, Y. Matsui, S. Suzuki, H. Shiromaru, K. Yamauchi and Y. Achiba, *J. Chem. Phys. Lett.*, 1991, **186**, 35; D. Dubois, M. T. Jones and K. M. Kadish, *J. Am. Chem. Soc.*, 1992, **114**, 6446.
- R. Hoffmann, *Angew. Chem., Int. Ed. Engl.*, 1982, **21**, 711.
- B. Knight, N. Martin, T. Ohno, E. Ortí, C. Rovira, J. Veciana, J. Vidal-Gancedo, P. Viruela and F. Wudl, *J. Am. Chem. Soc.*, 1997, **119**, 9871.
- C. Mealli, A. Ienco, E. B. Hoyt Jr. and R. W. Zoellner, *Chem. Eur. J.*, 1997, **3**, 958.

8/07500J